THE ASTROPHYSICAL JOURNAL, 438:921–931, 1995 January 10

THE TEMPORAL EVOLUTION OF THE 1–5 MICRON SPECTRUM OF V1974 CYGNI (NOVA CYGNI 1992)

CHARLES E. WOODWARD[1,2,3]
Wyoming Infrared Observatory, Department of Physics and Astronomy, University of Wyoming, Laramie, WY 82071-3905
chelsea@wapiti.uwyo.edu

MATTHEW A. GREENHOUSE[2,3]
Laboratory for Astrophysics, MRC 321, National Air and Space Museum, Smithsonian Institution, Washington, DC 20560
matt@wright.nasm.edu

R. D. GEHRZ
Department of Astronomy, School of Physics and Astronomy, 116 Church Street SE, University of Minnesota, Minneapolis, MN 55455
gehrz@ast1.spa.umn.edu

Y. J. PENDLETON[3]
NASA Ames Research Center, Space Sciences Division, MS 245-3, Moffett Field, CA 94035
pendleton@prometheus.arc.nasa.gov

R. R. JOYCE
Kitt Peak National Observatory, P.O. Box 26732, Tucson, AZ 85726[4]
joyce@noao.edu

D. VAN BUREN[2]
California Institute of Technology, Pasadena, CA 94305
dave@ipac.edu

J. FISCHER[3]
Naval Research Laboratory, Remote Sensing Division, Code 7213, Washington, DC 20375
jfischer@irfp1.nrl.navy.mil

N. J. JENNERJOHN[3]
Department of Physics, San Francisco State University, San Francisco, CA 94037

AND

C. D. KAMINSKI
NASA-IRTF, 2680 Woodlawn Drive, Honolulu, HI 96822
Received 1994 June 8; accepted 1994 July 18

ABSTRACT

We present 1–5 μm moderate- and high-resolution infrared spectra of the ONeMg nova V1974 (Nova Cygni 1992) obtained at multiple epochs during an $\approx$500 day period after outburst. During the first 80 days, the spectra exhibited continuum emission from thermal bremsstrahlung (free-free radiation) with prominent recombination line emission from hydrogen, helium, nitrogen, and oxygen. The measured FWHM of these recombination lines suggests that the initial velocity of the ejecta was $\approx$2400–3400 km s^{-1}. We estimate from the hydrogen recombination line ratios that the density of the ionized shell at this epoch was $\approx 10^9$ cm^{-3}, with an effective electron temperature of $\approx 5 \times 10^3$ K. As the temporal evolution of the ejecta progressed, the hydrogen and helium lines diminished in intensity, and coronal lines of aluminum, calcium, magnesium, neon, and sulfur appeared by $\approx$day 80. The coronal line emission phase persisted for over 400 days. During this epoch, no significant dust formation occurred. We find that the ejecta of V1974 Cyg were overabundant in aluminum *with respect to silicon* by a factor of $\approx$5 and in magnesium *with respect to silicon* by a factor of $\geq$3 relative to the solar photosphere. Comparison of our observed overabundances with recent model predictions of elemental synthesis in ONeMg outbursts suggests that the accreted envelope on V1974 Cyg was close to solar composition and that the precursor ONeMg white dwarf had a mass of $\approx 1\ M_\odot$.

Subject headings: infrared: stars — novae, cataclysmic variables — stars: abundances — stars: individual (Nova Cygni 1992)

1. INTRODUCTION

Infrared studies of classical nova outbursts provide information about the nature of the dust and gas they eject into the interstellar medium. In particular, infrared spectroscopy of novae can provide fundamental information about the abundances of gas phase elements and the physical conditions in nova ejecta (Gehrz 1990; Gehrz, Truran, & Williams 1993). The observed chemical abundances in the ejecta are end pro-

[1] Presidential Faculty Fellow.
[2] Visiting Astronomer, Kitt Peak National Observatory, National Optical Astronomy Observatories, operated by the Association of Universities for Research in Astronomy, Inc., under cooperative agreement with the National Science Foundation.
[3] Visiting Astronomer, NASA Infrared Telescope Facility, operated by the University of Hawaii, under contract with the National Aeronautics and Space Administration.
[4] Operated by the Association of Universities for Research in Astronomy, Inc., under cooperative agreement with the National Science Foundation.

ducts of the thermonuclear runaway (TNR) reactions occurring on the surface of the white dwarf and depend upon the history of mass transfer and accretion in the binary system, the white dwarf interior chemical composition, and the mass of the nova progenitor (Starrfield et al. 1992b; Starrfield, Sparks, & Truran 1986).

After TNR detonation occurs, an expanding pseudo-photosphere is ejected from the nova. As this material becomes optically thin, the 1–5 μm energy distributions are dominated by recombination lines, primarily of hydrogen and helium, that diminish in intensity as the nova evolves. Subsequent to this period, many novae exhibit a "coronal line" emission phase whose onset occurs from tens to hundreds of days after outburst (Greenhouse et al. 1988, 1990; Benjamin & Dinerstein 1990). Infrared coronal lines are low excitation temperature ($10^3 \leq T_{excit}(K) \leq 10^5$), high critical density ($10^6 \leq n_{crit}(cm^{-3}) \leq 10^9$) forbidden-line transitions of heavy ions with ionization potentials of ≥ 100 eV (cf. Greenhouse et al. 1993) and are frequently prevalent in the spectra of ONeMg novae.

Nova Cygni 1992 (V1974 Cyg) was discovered on 1992 February 19 (Collins 1992). This was the brightest nova outburst ($V_{max} \approx +4.3$ mag) in the last two decades in the northern hemisphere. We adopt 1992 February 19 UT (JD 2,448,671) as day 0 for V1974 Cyg. Since its outburst, V1974 Cyg has been the subject of dedicated study from γ-ray through radio wavelengths. In particular, the detection of neon emission from the ejecta ≈ 54 days after outburst (Gehrz et al. 1992a) suggested that the spectral evolution of V1974 Cyg would be similar to that of the archetypal ONeMg Nova QU Vulpeculae 1984 No. 2 (Greenhouse et al. 1988; Gehrz, Grasdalen, & Hackwell 1985). These novae are characterized in part by strong [Ne II] 7.6 μm and [Ne II] 12.8 μm emission that peaks within a few months after outburst (Gehrz et al. 1994b, hereafter Paper I). Optical spectra of ONeMg novae exhibit strong [Ne V] emission at wavelengths shortward of 3400 Å (Dopita et al. 1994). Ultraviolet spectra show strong Mg II 2800 Å and both [Ne IV] 1602 Å and [Ne V] 1575 Å emission (Saizar et al. 1992). Abundance analyses of the material ejected by these novae show that oxygen, neon, aluminum, and magnesium are enhanced over a solar abundance. Derived abundances from the ultraviolet and infrared neon emission lines show that the ejecta of V1974 Cyg was significantly overabundant in neon, by a factor of ≈ 4 (Hayward et al. 1992) to 10 (Paper I; Saizar et al. 1992) with respect to the solar photosphere, while being depleted in hydrogen (Hauschildt et al. 1994).

Helium line ratios measured in optical spectra indicated a reddening of $E(B-V) \simeq 0.3$, which suggested a distance of 1–2 kpc if V1974 Cyg radiated at the Eddington luminosity for a 1 $M_\odot$ white dwarf (Austin et al. 1992; Shore et al. 1992b) at maximum light. Direct measurement of the angular expansion rate of the shell (≈ 0.28 milliarcsec day^{-1}) obtained from *Hubble Space Telescope* (*HST*) observations yielded a minimum distance of ≈ 3.2 kpc, assuming an average expansion velocity of ≈ 1500 km s^{-1} (Paresce 1993). For the discussion which follows, we adopt a distance of 3.2 kpc. At this distance, V1974 Cyg is the closest ONeMg nova yet discovered.

The infrared light curve of V1974 Cyg has decayed slowly, and the nova has formed little dust. This slow evolution has permitted us to conduct a lengthy spectrophotometric monitoring program of this nova. Results of our mid-infrared spectroscopic observations are presented in Paper I and in Hayward et al. (1992), while the temporal evolution of the broadband infrared light curves are discussed in Woodward et al. (1994, hereafter Paper III). In this paper (Paper II of the series), we summarize our near-infrared ground-based spectroscopy of V1974 Cyg obtained at various epochs during the ≈ 500 day period after outburst and discuss the nova's evolution, including the temporal development of the line emission, the elemental abundances, and the mass of gas seen in coronal emission.

2. OBSERVATIONS

The 1–5 μm spectra presented here were obtained during the period 1992 March 12–1993 June 4 on the Kitt Peak National Observatory (KPNO) 2.1 m telescope and during the period 1992 May 29–October 18 on the NASA Infrared Telescope Facility (IRTF) 3 m telescope. The near-infrared spectra are presented in Figures 1–12.

The KPNO data were obtained with the cryogenic imaging spectrometer (CRSP) with a 58 × 62 InSb focal-plane array (Joyce, Fowler, & Heim 1994) using either a $\approx 1''.7$ or 3″ slit. Multiple spectra at a particular grating setting and spectral resolution (0.0012 μm pixel$^{-1} \leq \Delta\lambda/\lambda \leq 0.0022$ μm pixel^{-1}) were obtained by stepping the source along the slit at $\approx 5''$–7″ intervals. Photometric standards were observed in a similar manner. The two-dimensional spectral images of both the nova and photometric calibration stars were processed using standard infrared techniques (cf. Joyce 1992). Background images used for the first-order removal of night-sky emission from individual source images were generated by median-filtering all images in a given observational set. Individual one-dimensional spectra were subsequently extracted from each image using the IRAF APEXTRACT package. Final spectra were generated by averaging the extracted spectra and scaling each spectrum to the median of the total co-added data set.

Flux calibration was performed by using the spectra of photometric standard stars that were convolved with a blackbody source function appropriate to their known spectral type.

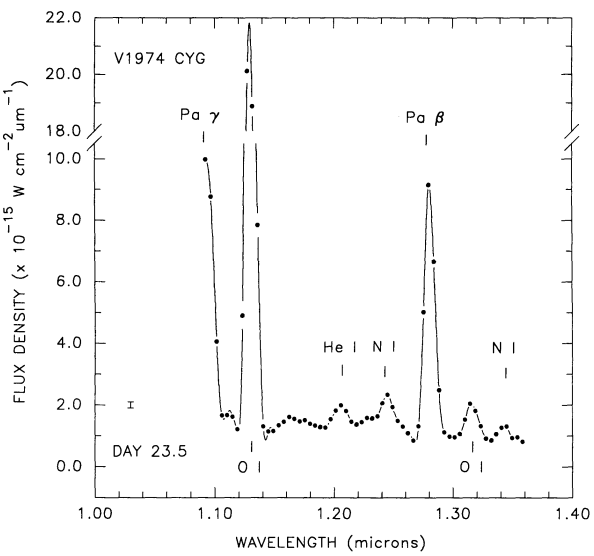

FIG. 1.—Low spectral resolution 1.08–1.36 μm spectrum (J band) of V1974 Cyg obtained on day 23.5 (1992 March 12.5 UT) from the KPNO 2.1 m telescope (+CRSP). Prominent spectral features are recombination lines of helium and hydrogen (Paschen series), as well as emission from oxygen and nitrogen. A representative 1 σ error is given at the lower left of the panel, and a cubic spline has been drawn through the data points as a visual aid.

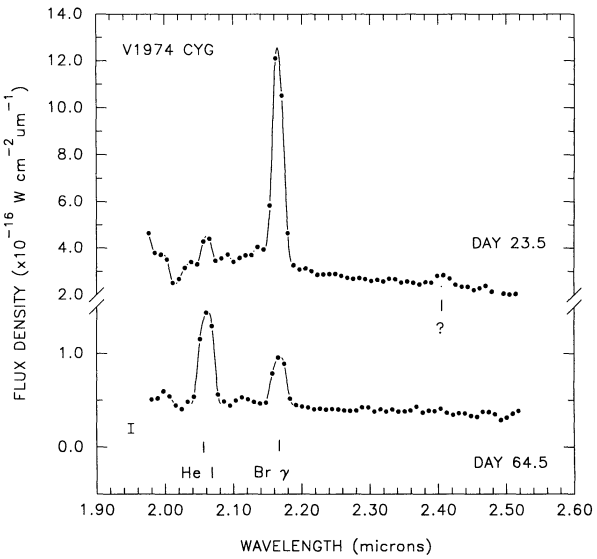

FIG. 2.—Low spectral resolution 1.96–2.54 μm spectra (K band) of V1974 Cyg obtained during two different epochs, day 23.5 (1992 March 12.5 UT) and day 64.5 (1992 April 22.5 UT) from the KPNO 2.1 m telescope (+CRSP). Hydrogen and helium recombination lines are prominent. The intensity of the hydrogen emission lines diminished by a factor of $\gtrsim 5$ as the ejecta evolved over this ≈ 40 day period. A representative 1 σ error bar is given at the lower left of the panel, and a cubic spline has been drawn through the data points as a visual aid.

The blackbody was normalized to the 2.2 μm flux density derived from a Kurucz (1979) model atmosphere. Residual absorption from hydrogen recombination lines in the stellar spectra were removed by a linear interpolation of the continuum adjacent to the features prior to division of the object spectra. Precise wavelength calibration was determined from

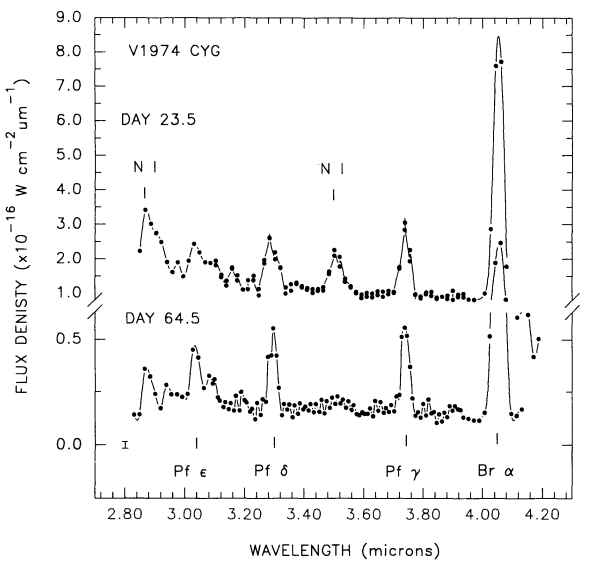

FIG. 3.—Low spectral resolution 2.80–4.20 μm spectra (L band) of V1974 Cyg obtained during two different epochs, day 23.5 (1992 March 12.5 UT) and day 64.5 1992 April 22.5 UT) from the KPNO 2.1 m telescope (+CRSP). Prominent spectral features are the hydrogen recombination lines of the Pfund series as well as Brα. The broad unidentified line at 3.450 μm was not detected in any spectra obtained after day 64.5. The weak feature on the red wing of the Pfϵ line is attributed to a helium emission line (see Fig. 7). A representative 1 σ error bar is given at the lower left of the panel, and a cubic spline has been drawn through the data points as a visual aid.

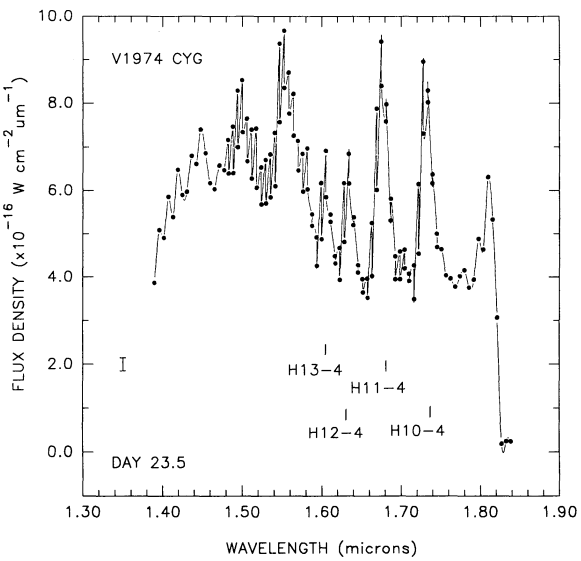

FIG. 4.—Low spectral resolution 1.36–1.86 μm spectrum (H band) of V1974 Cyg obtained on day 23.5 (1992 March 12.5 UT) from the KPNO 2.1 m telescope (+CRSP). Prominent spectral features are Brackett series hydrogen lines. A representative 1 σ error bar is given at the lower left of the panel, and a cubic spline has been drawn through the data points as a visual aid.

the strong emission lines present in the nova spectra and from telluric emission features present in sky spectra. No atmospheric extinction corrections were made to the data, since V1974 Cyg and comparison photometric standards were observed at comparable air masses.

The IRTF spectra were obtained using the cooled grating array spectrometer (CGAS) with a 1 × 32 linear InSb focal-plane detector (Tokunaga, Smith, & Irwin 1987). Two gratings were used to obtain the observations of V1974 Cyg: a 75 line

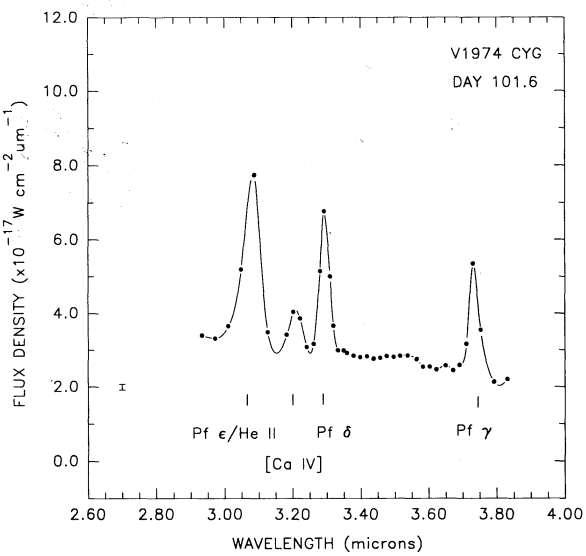

FIG. 5.—Low spectral resolution 2.80–3.90 μm spectrum (L band) of V1974 Cyg obtained on day 101.6 (1992 May 29.6 UT) from the NASA IRTF 3 m telescope (+CGAS). Prominent spectral features are Pfund series hydrogen lines as well as emission from Ca^{+3}. A representative 1 σ error bar is given at the lower left of the panel, and a cubic spline has been drawn through the data points as a visual aid. Observations shortward of 3.20 μm were affected by strong telluric features. Data near these wavelengths were removed from the final spectra.

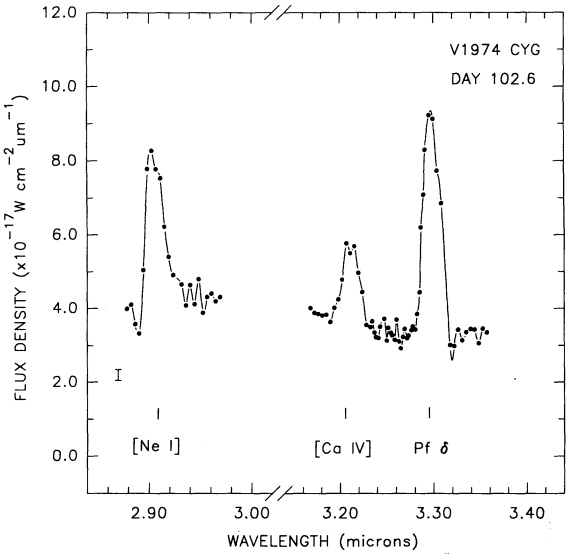

FIG. 6.—High spectral resolution 2.88–3.38 μm composite spectrum (derived from observations at two grating positions) of V1974 Cyg obtained on day 102.6 (1992 May 30.6 UT) from the NASA IRTF 3 m telescope (+CGAS). Prominent spectral features are the Pfδ hydrogen recombination line, [Ne I], and [Ca IV]. A representative 1 σ error bar is given at the lower left of the panel, and a cubic spline has been drawn through the data points as a visual aid.

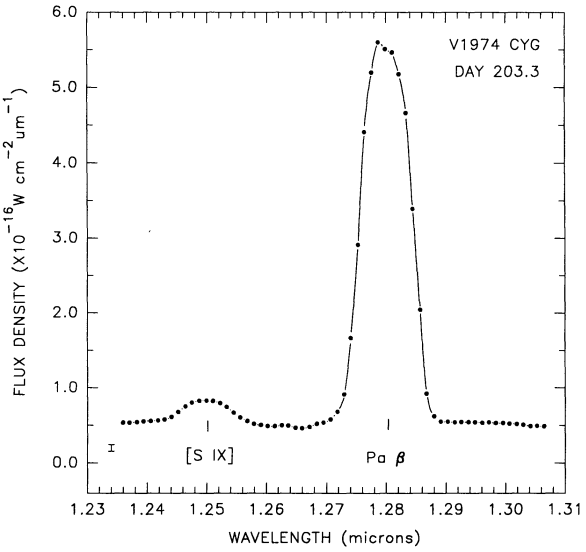

FIG. 8.—High spectral resolution 1.260–1.360 μm spectrum of V1974 Cyg obtained on day 203.3 (1992 September 08.3 UT) from the KPNO 2.1 m telescope (+CRSP). Prominent spectral features are the Paβ hydrogen recombination lines and the $2s^22p^4\,{}^3P_2 \rightarrow {}^3P_1$ transition of [S IX]. This transition of sulfur had not previously been reported in any astronomical source. A representative 1 σ error bar is given at the lower left of the panel, and a cubic spline has been drawn through the data points as a visual aid.

mm^{-1} grating which provided a resolution of 0.018 μm per detector element ($\lambda/\Delta\lambda$ = 160–210 over a 2.80–3.61 μm wavelength interval) and a 300 line mm^{-1} grating which provided a resolution of 0.004 μm per detector ($\lambda/\Delta\lambda$ = 790–880 over a 3.25–3.55 μm wavelength interval). Both gratings were used in first order. Wavelength calibration was achieved by observations of argon lamp lines. The detector spacing on the one-dimensional CGAS array provides one detector per resolution element. Nyquist sampling of the spectra was performed by moving the grating by fractions of a resolution element. The CGAS beam size was 2".7, and telluric emission was subtracted by chopping to reference positions 100" north and south of the nova. Corrections for atmospheric absorption and flux calibration were accomplished by comparison with nearby bright stars whose spectra were measured through similar air masses on the same night as the program object (usually within an

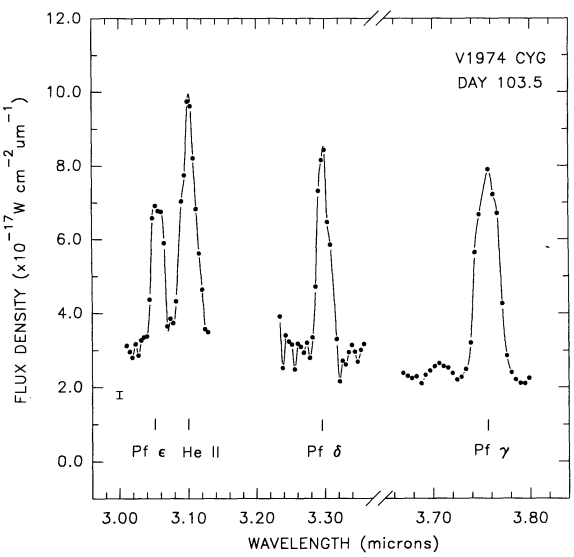

FIG. 7.—High spectral resolution 3.00–3.88 μm composite spectrum (derived from observations at three grating positions) of V1974 Cyg obtained on day 103.5 (1992 May 31.5 UT) from the NASA IRTF 3 m telescope (+CGAS). Prominent spectral features are the Pfund series hydrogen recombination lines and He II. A representative 1 σ error bar is given at the left of each spectral segment, and a cubic spline has been drawn through the data points as a visual aid.

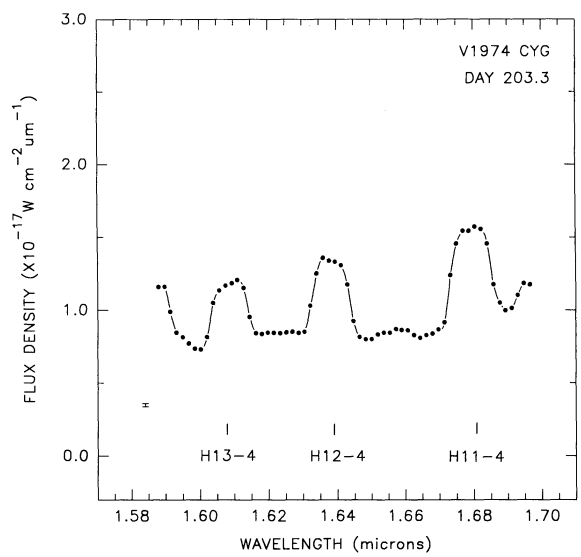

FIG. 9.—High spectral resolution 1.590–1.700 μm spectrum of V1974 Cyg obtained on day 203.3 (1992 September 08.3 UT) from the KPNO 2.1 m telescope (+CRSP). Prominent spectral features are the Paschen series hydrogen recombination lines. A representative 1 σ error bar is given at the lower left of the panel, and a cubic spline has been drawn through the data points as a visual aid.

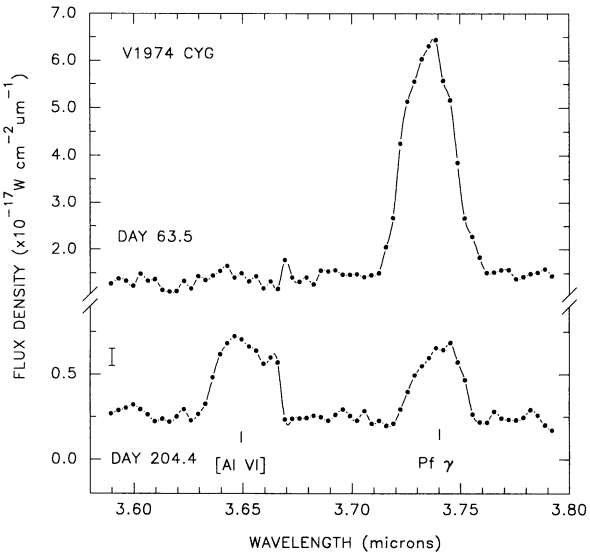

FIG. 10.—High spectral resolution 3.640–3.790 μm spectra of V1974 Cyg obtained during two different epochs, day 63.5 (1992 April 21.5 UT) and day 204.4 (1992 September 09.4 UT) from the KPNO 2.1 m telescope (+CRSP). Only the Pfγ hydrogen recombination line is evident in the day $\approx$63 spectrum. However, $\approx$141 days later the coronal line [Al VI] was observed, confirming that near this epoch V1974 Cyg had entered into the coronal line phase of its evolution $\approx$200 days after outburst. This evolutionary timescale is comparable to that seen in other novae that have exhibited coronal line emission, such as DK Lac or PW Vul. A representative 1 σ error bar for each spectrum is given at the right, and a cubic spline has been drawn through the data points as a visual aid.

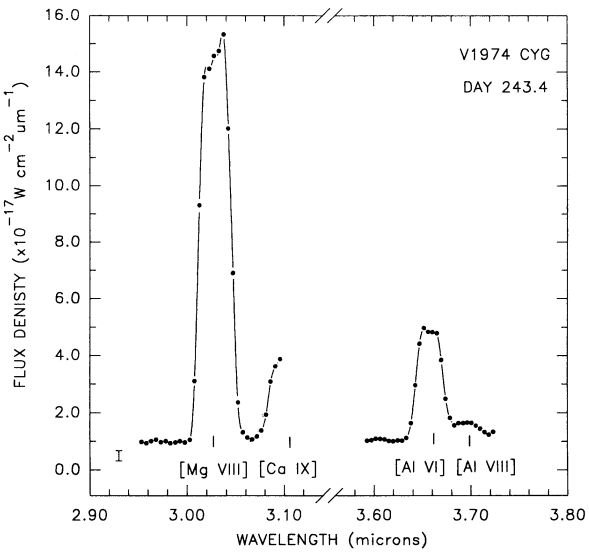

FIG. 11.—High spectral resolution 2.940–3.740 μm composite spectrum (derived from observations at two grating positions) of V1974 Cyg obtained on day 243.4 (1992 October 18.4 UT) from the NASA IRTF 3 m telescope (+CGAS). Prominent spectral features are infrared coronal lines [Mg VIII], [Al VI], and [Al VIII]. We interpret the feature at 3.091 μm as the $3s3p\,^3P_1 \rightarrow {}^3P_2$ transition of [Ca IX]. The [Mg VIII] and [Al VI] lines observed during this epoch are velocity-resolved at 2600 km s^{-1} FWHM, indicating that no appreciable deceleration of the ejecta had occurred since the onset of the optically thin emission-line phase (Fig. 1). The increase in the [Al VI] intensity from day 204.4 (Fig. 10) and the large [Mg VIII]/[Al VI] intensity ratio observed on day 243.4 suggest that the coronal line phase was near maximum. A representative 1 σ error bar is given at the left of each spectral segment, and a cubic spline has been drawn through the data points as a visual aid.

hour). No further telluric extinction corrections were made to the data, since V1974 Cyg and comparison photometric standards were observed at comparable air masses.

3. DISCUSSION

The spectra of V1974 Cyg at all epochs showed continuum emission from thermal bremsstrahlung (free-free radiation) with superposed emission lines. During the 500 day period encompassing our spectroscopic observations, the evolution of the broadband 1–10 μm colors suggested that the ejecta of V1974 Cyg were optically thin, with no evidence for substantial dust shell formation (Woodward et al. 1992a; Gehrz, Lawrence, & Jones 1992b; Woodward & Gehrz 1992). Thus, a significant contribution to the observed near-infrared contin-

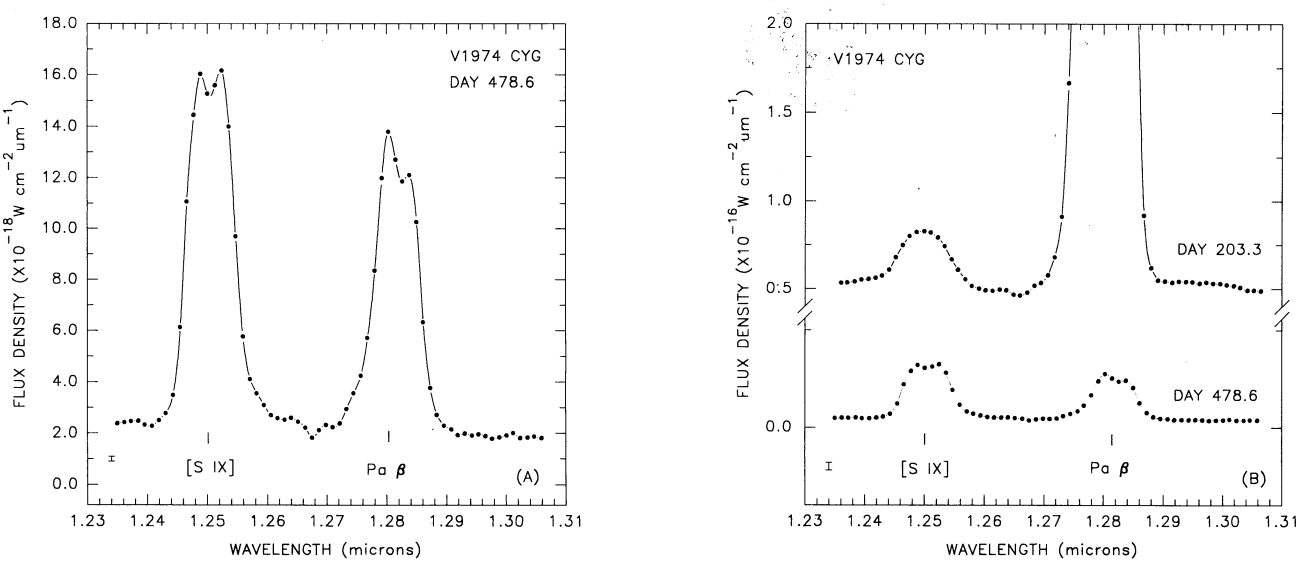

FIG. 12.—High spectral resolution 1.260–1.360 μm spectrum of V1974 Cyg obtained on day 478.6 (1993 June 4.3 UT) from the KPNO 2.1 m telescope (+CRSP). Prominent spectral features are the Paβ hydrogen recombination line and [S IX], which is of comparable integrated intensity. (*b*) Comparison spectra over the same wavelength range obtained during two different epochs, day 203.3 and day 478.6. Notice the dramatic decline in the Paβ line, and the rise in the [S IX] coronal line emission. A representative 1 σ error bar is given at the lower left of the panel, and a cubic spline has been drawn through the data points as a visual aid.

uum from thermally radiating dust is unlikely. The spectral lines observed in the nova included hydrogen and helium recombination lines, permitted lines of oxygen and nitrogen, and infrared coronal lines of [Al VI], [Al VIII], [Ca IV], [Ca IX], [Mg VIII], and [S IX]. Our discovery of the $2s^2 2p^4\ ^3P_2 \rightarrow\ ^3P_1$ line of [S IX] 1.250 μm and the $3s3p\ ^3P_1 \rightarrow\ ^3P_2$ lines of [Ca IX] 3.091 μm in V1974 Cyg marks the first identification of these lines in an astronomical source. Integrated line fluxes, derived from Gaussian fits, for lines that are clearly identified in our spectra are presented in Table 1. The statistical uncertainties in the derived line fluxes were estimated from the uncertainties in the observed flux densities but do not include possible systematic uncertainties caused by uncertainties in the instrument profile.

From day 23 through day 65, the dominant emission lines in the 1.10–1.35 μm (J band) spectra included hydrogen Paschen lines (Paγ, Paβ) and permitted lines of O I near 1.129 and 1.317 μm, and N I near 1.246 and 1.344 μm (Fig. 1). From 1.40 to 4.50 μm (H, K, and L bands) the hydrogen Brackett (H $n \rightarrow 4$) and Pfund (Pfγ, Pfϵ, Pfδ) recombination series lines were present, as well as the 2.058 μm helium emission line (Figs. 2–4; Fig 9). By day 100, the hydrogen and helium emission lines had declined in intensity, while emission from calcium and neon appeared (Figs. 5–7). During this epoch, lines attributed to [S IV] 10.51 μm and [S III] 18.71 μm tentatively were identified in 7.5–22.5 μm spectra (Emerson & Manning 1992). On day 150, rapid strengthening of emission from [Ne V] 3346, 3426 Å was observed in optical spectra (Barger et al. 1993).

A strong feature near 3.5 μm also was evident in the spectra obtained on day 23.5. However, within 21 days this feature was undetectable (Fig. 3). An emission feature at this wavelength, which faded rapidly in intensity, was observed in three other novae which formed little or no dust, including V1500 Cyg (Grasdalen & Joyce 1976), GQ Muscae (Krautter et al. 1984), and PW Vul 1984 (Evans et al. 1990). Krautter et al. (1984) attributed this feature to emission from polyformaldehyde (H_2CO_n). However, Evans et al. (1990) suggested that emission from N I is a more probable identification. Since other emission lines of nitrogen were present in our spectra of V1974 Cyg at this early epoch (Fig. 1), we concur with the identification of the 3.5 μm feature as arising from neutral nitrogen. Enhancement of nitrogen in nova ejecta is expected from TNR models on white dwarfs (Starrfield et al. 1992a).

The onset of a coronal line phase in V1974 Cyg was confirmed with our discovery of [S IX] 1.250 μm (possibly blended with He I) and [Al VI] 3.648 μm (Woodward et al. 1992b; Greenhouse et al. 1992) on $\approx$day 200 (Figs. 8 and 10). Spectroscopic observations by Dinerstein & Benjamin (1994) during this same epoch showed that the K-band spectrum of the nova ejecta changed dramatically from a recombination line–dominated spectrum on day 184 to a coronal line spectrum on day 203. Subsequent observations near 3 μm on day 243 (Fig. 11) revealed coronal line emission from even higher ionization species, including [Mg VIII] 3.028 μm, [Ca IX] 3.091 μm, and [Al VIII] 3.720 μm. During this period the ratio of the continuum to H I and He I lines in the K band increased by a factor of $\approx$2 (Dinerstein & Benjamin 1994). The increase in the observed ionization state of coronal line species and line-to-continuum ratios suggests that the ejecta were being photoionized by the hardening radiation field of the remnant.

The coronal phase in V1974 Cyg persisted at least 300 days. On day 478, [S IX] was dominant in the J-band spectrum, while Paβ had diminished in intensity by over a factor of 50 (Fig. 12). The temporal evolution observed in these spectra is similar to development of the mid-infrared hydrogen and neon emission lines (Paper I). In particular, the decline in the hydrogen recombination lines preceding and throughout the coronal line phase in V1974 Cyg is characteristic of infrared coronal line novae observed to date.

Appreciable deceleration of the ejecta of V1974 Cyg did not occur as it expanded into the interstellar medium, and the observed velocity dispersion suggested that this expelled material also was clumpy. Although the hydrogen emission line intensity declined as the ejecta evolved, the expansion velocity inferred from their line widths remained constant ($\approx$2500–3000 km s^{-1}) over the $\approx$500 days covered by our observations. This constant line width suggests that the bulk of the radiating gas had expanded at essentially constant velocity subsequent to being ejected from the white dwarf. Ultraviolet spectra (Shore et al. 1992a) and mid-infrared line profiles (Hayward et al. 1992) suggested that the ejecta of V1974 Cyg were distributed in clumps of varying ionization states exhibiting a range of outflow velocities. Multiple velocity components in the ejecta are clearly evident in the Hβ line profiles obtained on day 217 by Chochol et al. (1993) that show five distinct velocity components in the ejecta spanning $\approx$1700 km s^{-1}. Analysis of our observed hydrogen line ratios also indicate that clumps must be present in the ejecta of V1974 Cyg.

Nova ejecta are modeled to consist of dense, cool ($T_e \approx 10^4$ K) globules embedded in a hot ($T_e \approx 10^5$ K), tenuous confining medium (Saizar & Ferland 1994). The coronal line emitting region is believed to arise on the surfaces of cool globules that are photoionized by the nova remnant or by free-free radiation from the hot phase of the ejecta. The relative contribution of these two mechanisms to the total coronal line emission is unknown. In the case of V1974 Cyg, the coronal line width remained constant over a $\approx$500 day period. This trend suggests that the velocity dispersion among the globules remained constant or that the nova shell expanded at constant velocity without transferring appreciable momentum to ejecta from a previous outburst.

3.1. *Permitted* O I *Lines*

The TNR processes which result in a nova can substantially enrich the ejected envelope in carbon, nitrogen, and oxygen. Neutral oxygen was dominant in the J-band spectra of V1974 Cyg on day 23.5 (Fig. 1). A weaker feature attributed to O I at 1.316 μm also was detected. These lines are rarely seen in novae, especially with the intensities relative to Paβ observed in V1974 Cyg. Infrared emission from neutral oxygen has been identified in the spectra of four novae: Nova Aquilae 1993 (Woodward et al. 1993; Lynch et al. 1993), Nova Sagittarii 1992 No. 2 (Rossano et al. 1994), V1500 Cygni (Strittmatter et al. 1977), and the symbiotic nova V1016 Cygni (Rudy et al. 1990). Optical spectra of these novae obtained during the same epoch also exhibit a strong O I emission feature at 8446 Å. Emission from O I at 8446 Å was evident in the spectrum of V1974 Cyg on day 216 (Matheson, Filippenko, & Ho 1993).

The relative density of regions in the ejecta radiating the O lines and the excitation mechanism responsible for these permitted transitions can be deduced from the relative O I line fluxes. The presence of emission from neutral oxygen is important for understanding the ionization and density structure of the ejecta. The ionization potential of O I and H I are similar; thus regions which contain oxygen also should contain neutral hydrogen. Neutral oxygen is excited by three processes: recom-

TABLE 1

TEMPORAL DEVELOPMENT OF LINE FLUXES IN V1974 CYGNI

ION	WAVELENGTH (μm)	OBSERVED INTENSITY ($\times 10^{-19}$ W cm^{-2})									
		Day 23.5	Day 63.4	Day 64.5	Day 101.6	Day 102.6	Day 103.5	Day 203.3	Day 204.4	Day 243.4	Day 478.6
O I	1.110	2036.00 ± 305.70	...	...	...	...	...	...	...	...	
He I	1.206	95.00 ± 6.70	...	...	...	...	...	...	...	...	...
N I	1.246	98.92 ± 14.50	...	...	...	...	...	...	...	...	...
[S IX]	1.250	...	...	...	...	...	...	3.14 ± 0.19	...	...	1.22 ± 0.01
Paβ + He II	1.281	850.20 ± 84.94	...	...	...	...	...	49.28 ± 2.14	...	...	0.94 ± 0.03
O I	1.316	145.40 ± 8.45	...	...	...	...	...	...	...	...	...
N I	1.343	32.38 ± 0.77	...	...	...	...	...	...	...	...	...
H16–4	1.554	51.40 ± 8.34	...	...	...	...	...	...	...	...	...
H13–4	1.611	...	...	...	...	...	...	0.95 ± 0.09	...	...	...
H12–4	1.641	...	...	...	...	...	...	0.69 ± 0.05	...	...	...
[Si I]	1.659		...	...	...	...	...	0.09 ± 0.02	...	...	...
H11–4	1.677	83.95 ± 7.48	...	...	...	...	...	1.04 ± 0.13	...	...	...
H10–4	1.733	70.21 ± 6.66	...	...	...	...	...	...	...	...	...
He I	2.058	20.39 ± 8.79	...	27.11 ± 0.879	...	...	...	...	...	...	...
Brγ + He II	2.166	174.40 ± 11.101	...	12.66 ± 0.88	...	...	...	...	...	...	...
He II (13–8)	2.409	14.66 ± 2.20	...	...	...	...	...	...	...	...	...
[Ne I]	2.905	...	...	...	...	8.14 ± 2.22	...	...	...	...	...
[Mg VIII]	3.028		...	...	...	...	...	...	...	51.88 ± 4.10	...
Pfϵ	3.038	...	...	9.18 ± 0.93	...	...	7.74 ± 0.57	...	...	...	...
He II (7–6)	3.100	...	...	5.11 ± 0.85	...	...	14.30 ± 0.77	...	...	...	...
[Ca IX]	3.088	...	...	...	...	...	...	...	...	7.77 ± 1.42	...
[Ca IV]	3.211		...	...	3.28 ± 1.42	5.52 ± 0.15	...	...	...	...	...
Pfδ	3.296	60.13 ± 8.32	...	12.01 ± 0.62	12.44 ± 0.37	12.83 ± 0.15	11.55 ± 0.18	...	...	...	...
N I	3.507	55.90 ± 3.74	...	...	...	...	...	...	...	...	...
[Al VI]	3.661	...	...	...	...	...	...	...	1.30 ± 0.26	12.23 ± 0.51	...
[Al VIII]	3.720	...	...	...	...	...	...	...	...	1.71 ± 0.76	...
Pfγ	3.740	73.65 ± 3.92	13.98 ± 0.21	13.92 ± 0.72	12.32 ± 0.62	...	16.45 ± 0.20	...	1.05 ± 0.18	...	...
Brα + He II	4.052	311.30 ± 31.33	...	85.69 ± 0.75	...	...	...	...	...	...	...

bination, continuum fluorescence, and fluorescence by Lyβ. Detailed discussions of these mechanisms in astrophysical objects can be found in Grandi (1980, 1975) and Rudy, Rossano, & Puetter (1989 and references therein). We argue that the presence of O I in the spectrum of V1974 Cyg ≈ 20 days after outburst indicates that there were high-density ($n_e \approx 10^9$ cm^{-3}), neutral clumps initially present in the expanding nova envelope.

Comparison of the relative line fluxes of the observed infrared O I lines on day 23.5 suggests that Lyβ fluorescence was the primary excitation mechanism for neutral oxygen in the ejecta of V1974 Cyg during this epoch. Fluorescent excitation of O I by Lyβ photons results from the coincidence that Lyβ at 1025.72 Å can pump the O I ground-state $2p^4\,{}^3P$–$3d^3\,D^o$ line at 1025.77 Å (Bowen 1947). De-excitation of O I excited by absorption of a Lyβ photon can result in three photons at 11297, 8446, and 1304 Å (cf. Grandi 1980). Equal enhancement of these emission lines [resulting in $I(8446)/I(11297) \approx 1$] is distinctive of the Bowen fluorescence process. No measurement of 8446 Å line intensity on day 23.5 is available. Thus, we cannot assess whether the ratio of the photon fluxes, $I(8446)/I(11297)$, is near unity.

Continuum fluorescence of O I, in addition to producing weak optical lines of 7702 and 7254 Å, will give rise to a detectable line at 1.3164 μm. Although observed during different epochs, all three lines were evident in the spectra of V1974 Cyg. However, if continuum fluorescence was significant, the observed O I 1.3164 μm/1.1287 μm ratio would exceed unity (Grandi 1976). On day 23.5 the observed O I 1.3164 μm/1.1287 μm ratio was ≈ 0.07. Hence, the observed oxygen line ratios imply that the ejecta probably contained regions where both oxygen and hydrogen are neutral, yet the Lyβ flux density is high. In other novae, a small 1.3164 μm/1.1287 μm oxygen line ratio has suggested that ejecta densities exceed 10^9 cm^{-3} (Strittmatter et al. 1977; Rudy et al. 1990). The castellated pattern of the ultraviolet and mid-infrared emission-line profiles indicates that the ejecta of V1974 Cyg contain discrete condensations (Shore et al. 1992a; Hayward et al. 1992). The observed O I may arise from these warm, dense regions contained within a hotter ionized plasma. Analysis of the hydrogen recombination lines in § 3.2 confirms that high-density clumps existed in the ejecta of V1974 Cyg.

3.2. *Density and Temperature Estimates*

A variety of hydrogen lines were prominent in the spectra of V1974 Cyg during the ≈ 500 days covered by our observations. In principle, we can use the hydrogen line intensity ratios to infer an electron temperature and density. However, at our spectral resolution many of the observed hydrogen lines were blended with other lines, particularly those of helium [e.g., Paβ, 1.281 μm with He II ($10 \rightarrow 6$) 1.282 μm or Brγ 2.166 μm with He II ($14 \rightarrow 8$) 2.166 μm]. In addition, uncertainties in the absolute photometric calibration of spectra obtained with different grating settings and filter bandpasses contribute to uncertainty in the line flux ratios. However, in the low resolution L-band spectra obtained on days 23.4 and 64.5, both the Pfγ and Brα emission lines were observed simultaneously (Fig. 3). These lines are free of contaminating emission and are close in wavelength, so the effects of differential reddening are minimized even for values of A_V exceeding unity. Hayward et al. (1992) deduce a value of $A_V \approx 0.34$ toward V1974 Cyg. Adopting an extinction law similar to van de Hulst No. 15 (Willner & Pipher 1983), we conclude that the extinction optical depth τ at 4.0 μm is ≤ 0.012.

In the absence of appreciable line-of-sight extinction, the case B recombination Pfγ/Brα line intensity ratio was used to estimate upper limits to the electron temperature, T_e (K), and density, n_e (cm^{-3}), of the emitting plasma (cf. Osterbrock 1989). We have used values for these transitions of hydrogen tabulated by Hummer & Storey (1987). On day 23.5 the observed Pfγ/Brα ratio was 0.237 ± 0.023, consistent with $T_e \approx 5000$ K and $n_e \approx 10^{10}$ cm^{-3}. On day 64.5, Pfγ/Br$\alpha = 0.162 \pm 0.009$, suggesting that the density was $\approx 5 \times 10^9$ cm^{-3} if the ejecta evolved at constant temperature during this 41 day interval.

High-resolution H-band spectra obtained on day 203 (Fig. 9), after onset of the coronal line phase, exhibited clearly resolved H 13–4, H 12–4, and H 11–4 recombination lines. Thus, estimates of T_e and n_e are possible for this epoch. However, the case B line intensity ratios for these transitions, as a function of density at a given electron temperature, are nonunique and lead to an ambiguous estimate for n_e at densities $\geq 10^6$ cm^{-3}. The observed H 13–4/H 11–4 ratio (0.917 ± 0.143) is consistent with a day 203 density of $10^7 \leq n_e(\text{cm}^{-3}) \leq 10^9$ at $T_e = 10^3$ K. Given the observational uncertainty, we adopt a density of 10^7 cm^{-3} during this epoch.

The density range estimated above is consistent with that inferred by Hayward et al. (1992) for day 54, $n_e \approx 1.7 \times 10^{10}$ cm^{-3}, and for day 260, $n_e \approx 1.7 \times 10^7$ cm^{-3} (Paper I). Furthermore, the [O III] 4363 Å line intensity observed by Barger et al. (1993) at late stages of the nova evolution (day 450) suggests regions with densities exceeding 10^6 cm^{-3} Apparently V1974 Cyg ejected a dense shell of ionized gas with a relatively cool electron temperature. Evidence for a cool ($T_e \leq 10^4$ K) gas component in the principal ejecta of coronal line novae also was seen in the novae V827 Her and V1819 Cyg (Benjamin & Dinerstein 1990). However, Saizar & Ferland (1994) have demonstrated the existence of a hot ($T_e \approx 10^5$ K) component of the ejecta in the prototypical coronal line nova QU Vul.

3.3. *Ionization Temperature and Elemental Abundances*

Infrared coronal lines provide a primary means for determining elemental abundances in nova ejecta (cf. Greenhouse et al. 1990). Our measurement of [Al VI] 3.661 μm and [Mg VIII] 3.028 μm emission on day 243.4 (Table 1) enables us to constrain the relative abundance of these elements in V1974 Cyg. Using equation (3) of Greenhouse et al. (1993), we can express the line ratio I_{ij}/I_{kl} due to transitions $j \rightarrow i$ in ion X^{+p} and $l \rightarrow k$ in ion Y^{+q} as

$$\frac{I_{ij}}{I_{kl}} = \frac{A_{ij}}{A_{kl}} \frac{\lambda_{kl}}{\lambda_{ij}} \frac{n(\mathrm{X}_j^{+p})}{n(\mathrm{X}_{\mathrm{tot}}^{+p})} \frac{n(\mathrm{Y}_{\mathrm{tot}}^{+q})}{n(\mathrm{Y}_l^{+q})} \frac{n(\mathrm{X}_{\mathrm{tot}}^{+p})}{n(\mathrm{X})} \frac{n(\mathrm{Y})}{n(\mathrm{Y}_{\mathrm{tot}}^{+q})} \frac{n(\mathrm{X})}{n(\mathrm{Y})}, \quad (1)$$

where A is the spontaneous transition probability, $n(\mathrm{X}_j^{+p})/n(\mathrm{X}_{\mathrm{tot}}^{+p})$ is the relative population of the level j in the ion X^{+p}, $n(X^{+p})/n(X_{\mathrm{tot}})$ is the relative abundance of the ionization state p of element X, and $n(\mathrm{X})/n(\mathrm{Y})$ is the gas phase relative abundance of the elements X and Y.

We parameterize the fractional abundance of the ionization states $n(\mathrm{X}^{+p})/n(\mathrm{X}_{\mathrm{tot}})$ by an ionization temperature T_i using model coronal ionization equilibria (Shull & Van Steenberg 1982; Landini & Fossi 1972). We then use equation (1) and data from Greenhouse et al. (1993) to calculate [Mg VIII]/[Si VII] and [Al VI]/[Si VI] line ratios as a function of n_e and T_i assuming solar photospheric abundances for Mg, Al, and Si (Grevesse & Anders 1989). The results are shown in the upper panels of Figures 13 and 14.

We constrain T_i using measured [Si VI] 1.959 μm and [Si VII] 2.474 μm fluxes as shown in Figure 6 of Paper I. The critical density for collisional de-excitation above the silicon

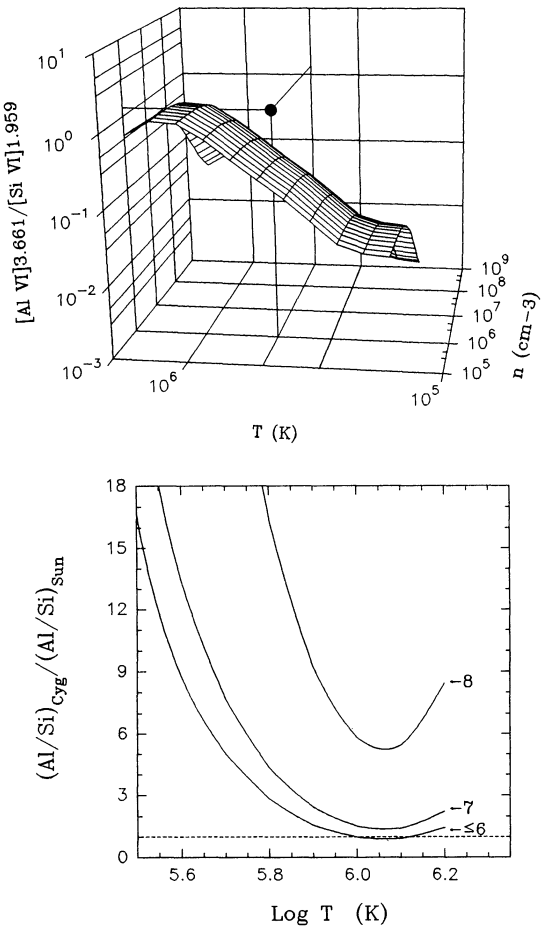

FIG. 13.—Predicted [Al VI] 3.661 μm/[Si VI] 1.959 μm line ratio as a function of electron density and ionization temperature, compared with measured value in V1974 Cyg. The surface shown in the upper panel was calculated using eq. (3) of Greenhouse et al. (1993) and solar photospheric abundances from Grevesse & Anders (1989). Selective extinction between the *L*- and *K*-band lines is ignored. The solid data point shown corresponds to a [Al VI] 3.661 μm measurement on day 243.4 (see Table 1) and is plotted at our derived density and temperature for this epoch (§ 3.3). The observed ratio lies above the surface, suggesting that V1974 Cyg was overabundant in Al with respect to Si relative to the solar photosphere. The lower panel shows the gas phase abundance of aluminum relative to silicon as a function of assumed electron density and ionization temperature. The curve labels are values of log n_e, and the dashed line denotes solar proportions of these elements.

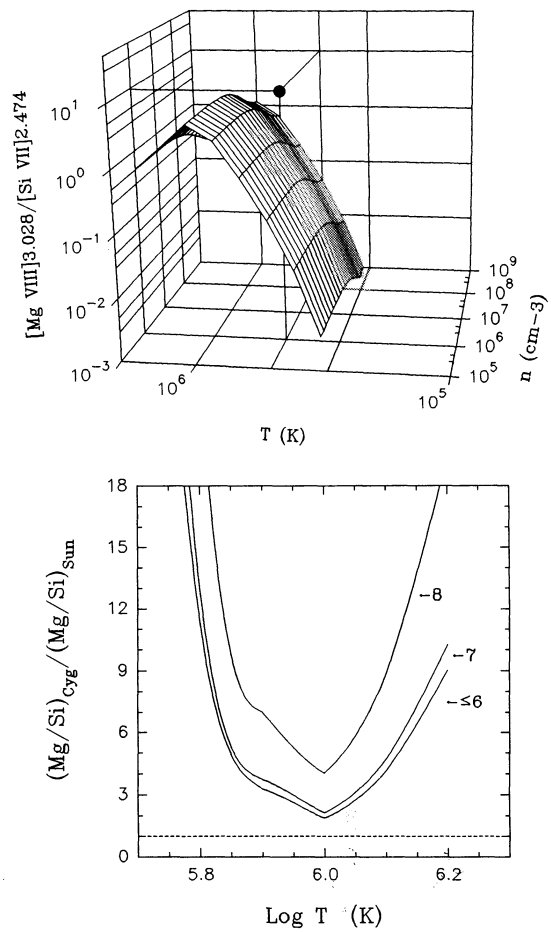

FIG. 14.—Predicted [Mg VIII] 3.028 μm/[Si VII] 2.474 μm line ratio as a function of electron density and ionization temperature, compared with a measured value in V1974 Cyg. The surface shown in the upper panel was calculated using eq. (3) of Greenhouse et al. (1993) and solar photospheric abundances from Grevesse & Anders (1989). Selective extinction between the *L*- and *K*-band lines is ignored. The solid data point shown corresponds to a [Mg VIII] 3.028 μm measurement on day 243.4 (see Table 1) and is plotted at our derived density and temperature for this epoch (§ 3.3). The observed ratio lies above the surface, suggesting that V1974 Cyg was overabundant in Mg with respect to Si relative to the solar photosphere. The lower panel shows the gas phase abundance of aluminum relative to silicon as a function of assumed electron density and ionization temperature. The curve labels are values of log n_e, and the dashed line denotes solar proportions of these elements.

transitions differs by a factor of 4, resulting in a density dependence on the derived ionization temperature. However, this dependence is weak below $n_e = 10^7$ cm^{-3} and is negligible for $n_e \leq 10^6$ cm^{-3}. Using data reported by Dinerstein et al. (1992), we derive a day 243 [Si VI] 1.959 μm/[Si VII] 2.474 μm intensity ratio of 1.8, yielding an ionization temperature range of $4.8 \leq T_i(10^5\ \mathrm{K}) \leq 4.9$ for densities in the range $10^5 \leq n_e(\mathrm{cm}^{-3}) \leq 10^7$, respectively. We can now compare the [Mg VIII] 3.028 μm/[Si VII] 2.474 μm and [Al VI] 3.661 μm/[Si VI] 1.959 μm line ratios expected for a solar mixture of Al, Mg, and Si with measured values in V1974 Cyg. The results are shown in the lower panels of Figure 13 and 14.

Abundances derived in this way depend on the assumed density and ionization equilibrium. The most reliable results are obtained when the species X^{+p} and Y^{+q} are chosen such that their characteristic ionization temperatures are nearly equivalent to each other and to the derived ionization temperature of the emitting region. One such example is [Ne VI] 7.642 μm and [Si VI] 1.959 μm (cf. Fig. 7 of Paper I). The comparisons shown in Figures 13 and 14 have somewhat higher dependence on T_i and relatively weak dependence on n_e.

In the case of aluminum (Fig. 13), we find that the day 243 line intensities would be consistent with a solar Al/Si abundance if ionization temperatures as large as 10^6 K were prevalent. However, our derived ionization temperature suggests that $(\mathrm{Al/Si})_{\mathrm{V1974\ Cyg}}/(\mathrm{Al/Si})_{\odot} \simeq 5$ for $n_e \leq 10^6$ cm^{-3}. In the case of magnesium (Fig. 14), the derivation is too temperature sensitive to deduce a specific value for Mg/Si. However, we find that, for any T_i, are measured line strength cannot be accounted for by solar proportions of Mg and Si in the ejecta. In this case we derive a lower limit of $(\mathrm{Mg/Si})_{\mathrm{V1974\ Cyg}}/(\mathrm{Mg/Si})_{\odot} \geq 3$ for $n_e \leq 10^6$ cm^{-3}.

We note that infrared coronal line transitions arise from relatively low energy terms. Consequently, they can be produced

in warm ($T_e \sim 10^4$ K $\ll T_i$) photoionized ejecta or not ($T_e \sim T_i$) collisionally ionized ejecta. Classical nova ejecta are modeled to contain warm photoionized globules surrounded by a hot coronal temperature medium (Saizar & Ferland 1994). It is unknown which conditions dominate the infrared coronal line region. However, it is likely that, in either extreme, coronal line emitting regions are inhospitable to grain formation. This assumption is consistent with the observed anticorrelation between dust and coronal line emission in novae (Gehrz et al. 1994a). As a result of this trend, and the absence of silicate grain features in the mid-infrared spectrum of V1974 Cyg, we conclude that the above elements are not appreciably depleted to such an extent that $(Si/H)_{V1974\ Cyg}/(Si/H)_\odot \simeq 1$.

3.4. *Heavy-Element Enrichment in V1974 Cyg*

V1974 Cyg was a fast nova (for a definition of speed class see Warner 1990), $t_3 \approx 16$ days, that exhibited heavy-element enrichment of Al, Mg, and Ne. Enrichment of these species in the ejecta is characteristic of fast novae (Truran & Livio 1986). In particular, the relative abundance of aluminum and sodium provides a useful test for models of TNR on ONeMg novae. Theoretical studies of TNR in the accreted envelopes of ONeMg white dwarfs predict that substantial amounts of ^{26}Al and ^{22}Na can be produced in nova explosions (Nofar, Shaviv, & Starrfield 1991; Starrfield et al. 1992b). However, the relative production rate of these two species is a strong function of the mass of the white dwarf progenitor, the temperature history of the TNR, and the composition of the nova envelope. Indeed, a strong anticorrelation between ^{26}Al and ^{22}Na production in nova outbursts has been suggested (Starrfield et al. 1992a). Verification of these hydrodynamic model predictions is important. Since the relative amounts of ^{22}Na and ^{26}Al depend strongly on the peak temperature reached in the explosion, measuring these abundances will constrain physical conditions of the TNR.

Upper limits of $\leq 7 \times 10^{-19}$ W cm^{-2} (3 σ) to the [Na III] 7.319 μm and [Na IV] 9.039 μm lines in V1974 Cyg were deduced from mid-infrared spectra obtained on day 242 (Paper I). Thus, sodium may not have a large abundance in the ejecta. Past determination of the sodium abundance in novae relied on the analysis of a nebular emission line at 2069 Å (Williams et al. 1985). However, it has been demonstrated recently that this line identification is incorrect (Shore et al. 1994). Observations of the mid-infrared sodium "coronal lines" are necessary to provide an accurate, unambiguous determination of the abundance. The large Al/Si ratio observed in V1974 Cyg is consistent with a Na/Si ratio near unity.

The observed abundance pattern of Al, Mg, and Si in V1974 Cyg is similar to that seen in other novae, independent of speed class. In Table 2 we summarize the abundance pattern $N(X)/N(Si)_{nova}$ relative to the solar photosphere (Grevesse & Anders 1989) for five novae which have published silicon abundances (cols. [2]–[5]). The modest enhancement (by a factor of ≈ 10) in the abundance of Al, Mg, and Ne in V1974 Cyg is similar to that observed in four of the five novae. In particular, comparison of the abundance pattern deduced for V1974 Cyg with recent models (Starrfield et al. 1992) suggests that the initial accreted envelope composition was nearly solar and that the outburst occurred on a white dwarf of intermediate mass $\approx 1\ M_\odot$. The wide range of Ne/Si abundance in the novae presented in Table 2 may indicate that neon enrichment arises from variations in the dredge-up mechanism of material into the ejected nova envelope from the underlying ONeMg white dwarf core (Nofar et al. 1991; Truran & Livio 1986).

4. CONCLUSIONS

V1974 Cyg is one of the few ONeMg coronal line nova to be studied spectroscopically in temporal detail at near-infrared wavelengths. Analysis of our 1–5 μm spectra obtained over a temporal baseline of ≈ 500 days since maximum light leads to several conclusions.

1. We have discovered the presence of [S IX] 1.250 μm and [Ca IX] 3.091 μm in V1974 Cyg, which have not been identified previously in novae.

2. The ratio Al/Si in V1974 Cyg was ≈ 5 times greater than the solar photospheric ratio, while Mg/Si was at least a factor of 3 times greater than the solar photospheric ratio. The observed abundance pattern suggests that the progenitor ONeMg white dwarf was of intermediate mass ($\approx 1\ M_\odot$) and that the initial accreted envelope of material was close to solar composition.

3. The hydrogen line intensity ratio suggests that the ejecta density exceeded 10^9 cm^{-3} on day 23.5 and 10^7 cm^{-3} on day 203. This ratio observed together with the presence of strong O I emission is evidence that the expanding ejecta was nonuniform in density and contained many clumps.

4. Our data suggest that the strong 3.507 μm emission feature present in the spectra of novae which form little or no dust can be attributed to emission from neutral nitrogen.

TABLE 2

ELEMENTAL ABUNDANCES IN CORONAL LINE NOVAE

$\frac{N(X)/N(Si)_{nova}}{N(X)/(N)(Si)_\odot}$ (1)	CrA 81[a] (2)	Aql 82[a] (3)	Cyg 75[b] (4)	QU Vul[b] (5)	V1974 Cyg (6)	Solar[c] $N(X)/N(Si)$ (7)
Al	24.1	...	≥ 2.5	≥ 6.7	≥ 5.0[d]	0.083
Na	14.9	...	...	...	≤ 1.0[d]	0.060
Ne	31.8	158.8	...	≥ 11.5	≥ 10.0[e]	3.467
Mg	3.7	8.4	≥ 5.0	≥ 4.9	≥ 3.0[d]	1.072
Speed class[f]	Fast	...	Fast	Slow	Fast	...

[a] Wiescher et al. 1986 and references therein.
[b] Greenhouse et al. 1990, corrected for revised solar abundances given in col. (7).
[c] From Grevesse & Anders 1989.
[d] See § 3.3 of this paper.
[e] Gehrz et al. 1994b (Paper I).
[f] After Warner 1990.

Note added in manuscript.—In Paper I (Gehrz et al. 1994b) the solar abundance $[n(\mathrm{Ne})/n(\mathrm{Si})]_{\odot}$ appears in § 3.1 incorrectly as 0.347. The correct value (Grevesse & Anders 1989) is 3.47. The error in the text is typographical and does not affect the results presented.

We are pleased to acknowledge the cooperation and support of the staff of NOAO and the NASA IRTF for their assistance with these observations. C. E. W. was supported by the National Science Foundation (AST 93-57392 and AST 91-16644) and the Research Office of the University of Wyoming. M. A. G. was supported in part by NASA grants NAG 1-711, NAG 2-880, and the Smithsonian Institution Scholarly Studies Program. R. D. G. was supported by the National Science Foundation, NASA, and the Graduate School of the University of Minnesota. We thank H. L. Dinerstein and R. A. Benjamin for their silicon line intensity data prior to publication, and S. Starrfield for many enlightening conversations.

REFERENCES

Austin, S. J., Starrfield, S., Wagner, R. M. Bertram, R., Peterson, B. M., & Houdashelt, M. 1992, IAU Circ., No. 5522
Barger, A. J., Gallagher, J. S., Bjorkman, K. S. Johansen, K. A., & Nordsieck, K. H. 1993, ApJ, 419, L85
Benjamin, R. A., & Dinerstein, H. L. 1990, AJ, 100, 1588
Bowen, I. S. 1947, PASP, 59, 196
Chochol, D., Hric, L., Urban, Z., Komzik, R., Grygar, J., & Papousek, J. 1983, A&A, 277, 103
Collins, P. 1992, IAU Circ., No. 5454
Dinerstein, H. L., & Benjamin, R. A. 1994, Rev. Mexicana Astron. Af., 27, 33
Dinerstein, H. L., Benjamin, R. A., Gaffney, N. I., Lester, D. F., & Ramseyer, T. F. 1992, BAAS, 24, 1189
Dopita, M., et al. 1994, ApJS, 93, 455
Emerson, J. P., & Mannings, V. 1992, IAU Circ., No. 5537
Evans, A., Callus, C. M., Whitelock, P. A., & Laney, D. 1990, MNRAS, 246, 527
Gehrz, R. D. 1990, in Physics of Classical Novae, ed. A. Cassatella & R. Viotti (Berlin: Springer-Verlag), 138
Gehrz, R. D., Grasdalen, G. L., & Hackwell, J. A. 1985, ApJ, 306, L49
Gehrz, R. D., Jones, T. J., Lawrence, G., Hayward, T. L., Houck, J., & Miles, J. 1992a, IAU Circ., No. 5497
Gehrz, R. D., Jones, T. J., Lawrence, G. F., & Woodward, C. E. 1994a, in preparation
Gehrz, R. D., Lawrence, G., & Jones, T. J. 1992b, IAU Circ., No. 5463
Gehrz, R. D., Truran, J. W., & Williams, R. E. 1993, in Protostars and Planets III, ed. E. Levy & J. Lunine (Tucson: Univ. Arizona Press), 75
Gehrz, R. D., et al. 1994b, ApJ, 421, 726 (Paper I)
Grandi, 1975, S. A. ApJ, 196, 462
———. 1976, Ph.D. thesis, Univ. Arizona
———.1980, ApJ, 238, 10
Grasdalen, G. L., & Joyce, R. R. 1976, Nature, 259, 187
Greenhouse, M. A., Feldman, U., Smith, H. A., Klapisch, M., Bhatia, A. K., & Bar-Shalom, A. 1993, ApJS, 88, 23
Greenhouse, M. A., Grasdalen, G. L., Hayward, T. L., Gehrz, R. D., & Jones, T. J. 1988, AJ, 95, 172
Greenhouse, M. A., Grasdalen, G. L., Woodward, C. E., Benson, J. A., Gehrz, R. D., Rosenthal, E., & Strutskie, M. F. 1990, ApJ, 352, 307
Greenhouse, M. A., Woodward, C. E., Fischer, J., & Smith, H. A. 1992 IAU Circ., No. 5674
Grevesse, N., & Anders, E. 1989, in AIP Conf. Proc. 183, Cosmic Abundances of Matter, ed. C. J. Waddington (New York: AIP), 1
Hauschildt, P. H., Starrfield, S., Austin, S., Wagner, R. M., Shore, S. N., & Sonneborn, G. 1994, ApJ, 422, 831
Hayward, T., Gehrz, R. D., Miles, J. W., & Houck, J. R. 1992, ApJ, 401, L101
Hummer, D. G., & Storey, P. J. 1987, MNRAS, 224, 801
Joyce, R. R. 1992, in ASP Conf. Ser. 23, Astronomical CCD Observations and Reduction Techniques, ed. S. B. Howell (Provo: Brigham Young Univ. Press), 258
Joyce, R. R., Fowler, A. M., & Heim, G. B. 1994, Proc. SPIE, 2198
Krautter, J., et al. 1984, A&A, 137, 307
Kurucz, R. L. 1979, ApJS, 40, 1
Landini, M., & Fossi, B. C. 1972, A&A, 7, 291
Lynch, D. K., Rossano, G. S., Rudy, R. J., & Puetter, R. C. 1993, BAAS, 25 (No. 4), 1378
Matheson, T., Filippenko, A. V., & Ho, L. C. 1993, ApJ, 418 L29
Nofar, I., Shaviv, G., & Starrfield, S. 1991, ApJ, 369, 440
Osterbrock, D. E. 1989, Astrophysics of Gaseous Nebulae and Active Galactic Nuclei (Mill Valley: University Science Books)
Paresce, F. 1993, IAU Circ., No. 5814
Rossano, G. S., Rudy, R. J., Puetter, R. C., & Lynch, D. K. 1994, AJ, 107, 1128
Rudy, R. J., Cohen, R. D., Rossano, G. S., & Puetter, R. C. 1990, ApJ, 362, 346
Rudy, R. J., Rossano, G. A., & Puetter, R. C. 1989, ApJ, 346, 799
Saizer, P., & Ferland, G. J. 1994, ApJ, 425, 755
Saizar, P., et al. 1992, ApJ, 398, 651
Shore, S. N., Ake, T. B., Starrfield, S., Sonneborn, G., Gonzales-Riestra, R., Kraemer, S., & Altner, B. 1992a, IAU Circ., No. 5614
Shore, S. N., Sonneborn, G., Starrfield, S., Gonzalez-Riestra, R., & Polidan, R. S. 1994, ApJ, 421, 344
Shore, S. N., Starrfield, S., Austin, S. J., Gonzales-Riestra, R., Sonneborn, G., & Wagner, R. M. 1992b, IAU Circ., No. 5523
Shull, J. M., & Van Steenberg, M. 1982, ApJS, 48, 95
Starrfield, S., Shore, S. N., Sparks, W. M., Sonneborn, G., Truran, J. W., & Politano, M. 1992a, ApJ, 391, L71
Starrfield, S., Sparks, W. M., & Truran, J. W. 1986, ApJ, 303, L5
Starrfield, S., Truran, J. W., Politano, M., Sparks, W. M., Nofar, I., & Shaviv, G. 1992b, in Proc. Workshop to Honor W. A. Fowler on His 80th Birthday, ed. S. Woosley, in press
Strittmatter, P. A., et al. 1977, ApJ, 216, 23
Tokunaga, A. T., Smith, R. G., & Irwin, E. 1987, in Proc. Workshop on Ground-based Astronomical Observations with Infrared Array Detectors, ed. C. G. Wynn-Williams & E. E. Becklin (Honolulu: Univ. Hawaii), 367
Truran, J. W., & Livio, M. 1986, ApJ, 308, 721
Warner, B. 1990, in Physics of Classical Novae, ed. A. Cassatella & R. Viotti (Berlin: Springer-Verlag), 24
Wiescher, M., Gorres, J., Thielemann, F.-K., & Ritter, H. 1986, A&A, 160, 56
Williams, R. E., Ney, E. P., Sparks, W. M., Starrfield, S., & Truran, J. W. 1985, MNRAS, 212, 753
Willner, S. P., & Pipher, J. L. 1983, 265, 760
Woodward, C. E., et al. 1993, BAAS, 25 (No. 4), 1378
Woodward, C. E., et al. 1992a BAAS, 24 (No. 4), 1189
Woodward, C. E., Van Buren, D., Hofner, P., & Greenhouse, M. A. 1992b, IAU Circ., No. 5612
Woodward, C. E., & Gehrz, R. D. 1992, IAU Circ., No. 5617
Woodward, C. E., Gehrz, R. D., Jones, T. J., Lawrence, G., & Skrutskie, M. 1994, in preparation (Paper III)